

# Valuable products from End of Life Vehicles (ELV) waste by thermal and thermo-catalytic degradation

J. Sója, N. Miskolczi and R. Nagy

MOL Department of Hydrocarbon and Coal Processing, University of Pannonia,  
Veszprém, 10 Egyetem st, 8200, Hungary

Corresponding author email address: sojajanos@almos.uni-pannon.hu, telephone  
number: +36 88 624 4410

## Abstract

The aim of this work is to study the catalytic effects of different ZSM-5 zeolite based catalysts during the thermo-catalytic pyrolysis in a stainless steel batch reactor at 425 °C and at 485 °C. Real ELV plastic waste as a raw material and the following catalysts were prepared by wet impregnation method was used: Zn/ZSM-5, Mg/ZSM-5, Fe(II)/ZSM-5, Sn/ZSM-5 and Ce/ZSM-5. The morphological characterization of catalysts was investigated by BET methods. Gas products of pyrolysis were determined by GC and the pyrolysis oils were analyzed by GC and FTIR. Application of Sn/ZSM-5 catalyst produced the maximum yield of pyrolysis oils and the minimum yield of gases in both cases. On the other hand, the lowest yield of pyrolysis oil and the highest yield of gas were found by the using of Ce/ZSM-5 catalyst. Gas products contain mainly C3-C5 hydrocarbons (88.7-91.9 wt%). Cerium-impregnated zeolite resulted the highest C1-2 hydrocarbons yield. In the liquid product the hydrocarbons were identified from C6 to C30. At both temperatures the most C30+ components generated with using of Sn/ZSM-5 catalyst. The pyrolysis oil contained mainly C6-C15 hydrocarbons (54.7-64.0 wt%). According to the results, Ce/ZSM-5 catalyst showed the highest catalytic cracking performance, and Sn/ZSM-5 catalyst showed the least.

## Keywords

End of Life Vehicles (ELV), waste recycling, pyrolysis, zeolite, catalysts

## 1. Introduction

Today our life is unimaginable without plastics. Since the population of the world is increasing, the demand for plastics is increasing as well. According to Plastics Europe, the worldwide plastic production was 322 million tons in 2015 [1]. The amount of plastic waste is rapidly growing and generating enormous economical problems. Obviously, something has to be done with the waste in order to reduce its disposal to the landfill. The best way would be the prevention of waste generation, however if waste has already produced they must be re-using, recycling or their energy has to be recovered. Waste to energy processes are good possibility for plastic waste utilization, because plastics have high energy content. Furthermore, the European Union promotes the waste recycling as a secondary raw material and valuable energy productions by various directives (e.g. 94/62/EC, 2000/53/EC) [2,3].

End of Life Vehicles (ELV) is a special plastic waste. In the European Union, every year 7-8 million tonnes ELV is produced only from passenger cars [4]. It is also known, that significant percentage of vehicle parts are plastic [5]. According to the 2000/53/EC directive from 1 January 2015, 95% of the waste coming from vehicles' construction material has to be utilized; 85 % by mechanical and 10 % by chemical recycling [3]. The biggest challenge with ELV recycling is their heterogeneous composition and contaminations. That is the reason for high cost consumption and difficult to implementation of ELV mechanical recycling. Chemical recycling, called as thermal and thermo-catalytic degradation could be a good option, because valuable products such as pyrolysis oil, flammable hydrocarbon gases, even hydrogen could be obtained [6-7]. These materials can be utilized for energy-production, or as feedstock for petrochemical and oil industry [8].

The pyrolysis is a thermochemical decomposition of organic material at elevated temperatures in the absence of oxygen. Shorter, less complex molecules with lower molecular weight could be obtained

from the long chain polymer molecules. Physical and chemical properties are significantly changing under this process. The three major products that are produced during pyrolysis are: gas, oil and solid coke-like residue. The products' yields and properties can be significantly affected by the reaction parameters. E.g. the conversion of decomposition could be increased by using different type of catalysts or by increased temperature [9-11]. Most widely zeolites are used as catalysts [9,12,13].

Many studies have been carried out on the catalytic thermal decomposition of different polymer wastes, biomass wastes or their various mixtures using ZSM-5 or metal-modified/ZSM-5 zeolite [14-22]. Wu et al. [16] investigated the hydrogen generating effect of the Ni/CeO<sub>2</sub>/ZSM-5 catalyst for the pyrolysis-gasification of polypropylene. They reported that 5 wt% CeO<sub>2</sub> content enhanced the hydrogen production, but much higher CeO<sub>2</sub> content (30 wt%) reduced the catalytic activity. Elbaba et al. [17] reported when the CeO<sub>2</sub> content was introduced into the Ni/Al<sub>2</sub>O<sub>3</sub> catalyst the hydrogen production increased and further increasing was observed when the CeO<sub>2</sub> content was grew from 5 to 15 wt%. However the further increase of the cerium-content to 30 wt% reduced the gas yield. Sun et al. [19] compared to the pyrolysis of biomass to aromatic hydrocarbons over ZSM-5 and Fe/ZSM-5 catalysts. It was found that the iron impregnated catalyst showed higher activity in formation of monocyclic aromatic hydrocarbons than the ZSM-5 catalyst. Wang et al. [21] studied the pyrolysis of fine pellets over Zn modified ZSM-5 catalyst in a microwave pyrolysis reactor. They reported that the bio-oil yield decreased while gas yield increased by adding zinc to zeolite, and the oil contained mostly aromatic hydrocarbons.

Our current work, thermo-catalytic pyrolysis of real ELV waste plastics was investigated by using different catalysts. Pyrolysis was taken place in a batch reactor at 425-485°C using modified commercial zeolite catalyst. To avoid the formation of unflavoured compounds (e.g. organic alcohols or ketones), nitrogen gas was used to ensure the inert atmosphere at ambient pressure. The used real ELV raw material (e.g. fuel tank, bumper, spoiler, interior part, etc.) contained mainly polyethylene and polypropylene. Different modified zeolite catalysts were synthesized by wet impregnation and used in 5% concentration to increase the yield of volatiles and reduce the heat consumption of the process. Gas products of pyrolysis were analyzed by GC and the liquid products were tested by GC and FTIR. Furthermore, the morphological characterization of catalysts was done by BET methods. It was concluded, that the catalysts have greatly influenced the composition of products. Gases have enough high heating values to support the energy consumption of pyrolysis.

## 2. Experimental

### 2.1. Raw materials

Real ELV plastic waste from Hungary was grinded to the size maximum 7 mm for experimental use. Its composition was investigated by Fourier-transformed infrared spectroscopy based on spectrum comparison. According to the results, the raw materials contained 41 % HDPE, 42 % PP and 17 % LDPE. Its volatile material content was 0.31 wt% and the ash content was 0.62 wt%.

### 2.2. Catalyst preparation

ZSM-5 catalyst was supplied by the MOL Plc and different catalysts were prepared by wet impregnation method: Zn/ZSM-5, Mg/ZSM-5, Fe(II)/ZSM-5, Sn/ZSM-5 and Ce/ZSM-5. For impregnation 1 M ZnSO<sub>4</sub>·7H<sub>2</sub>O, MgSO<sub>4</sub>·7H<sub>2</sub>O, FeSO<sub>4</sub>·7H<sub>2</sub>O, SnCl<sub>2</sub>·2H<sub>2</sub>O and Ce(SO<sub>4</sub>)<sub>2</sub>·4H<sub>2</sub>O solution were used, respectively. The compounds were dissolved in distilled water. Then ZSM-5 zeolites was added at 80 °C and stirred for 2 hours. Then zeolites were separated by centrifugation, washed several times, dried for 10 hours at 110 °C, and each of them was calcined at 600 °C for 3 hours.

### 2.3. Apparatus for pyrolysis

Pyrolysis was carried out in a stainless steel batch reactor. The layout of the used reactor can be seen on the Fig1. 50 g of raw materials and 5 m/m% modified zeolite catalysts were placed into the reactor. The reactor was fitted with electric heater and PID temperature controller. The reaction temperature is

measured by two type K thermocouples, placed in the raw material and catalyst mixture, and at the external wall, respectively. The pyrolysis was performed at 425 and at 485 °C. To avoid the formation of undesirable compounds (e.g. organic alcohols or ketones), nitrogen gas (11 dm<sup>3</sup>/h) was used to ensure the inert atmosphere at ambient pressure. Firstly the raw materials had been decomposed in the reactor and then volatiles hydrocarbons were condensed in a water cooled heat exchanger that was kept at 40 °C. Then products were separated into gas fraction and pyrolysis oil in a phase separator. The volume of the hydrocarbon gases was measured by gas flow meter. The solid fraction contained the carbonaceous char and the catalyst.

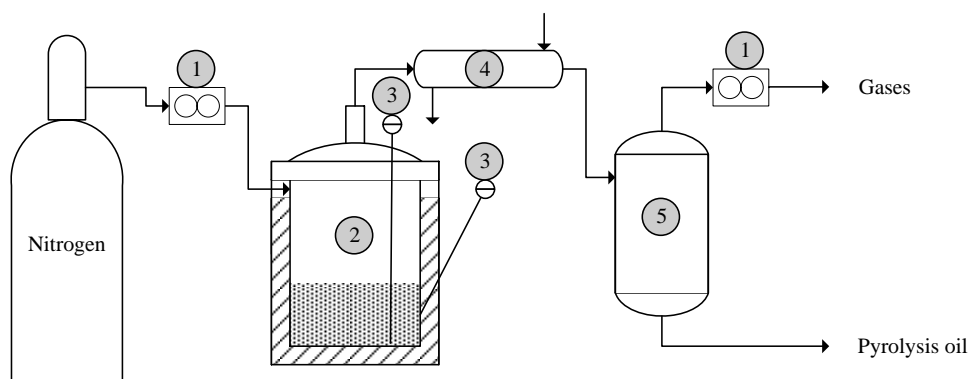


**Fig1** Simplified layout of the pyrolysis reactor (1 – gas flow meter, 2 - electrically heated reactor, 3 - thermocouples, 4 – water cooled condenser, 5 – phase separator)

## 2.4. Methods for analysis

The chemical structure of pyrolysis oil was monitored by FTIR spectroscopy. A TENSOR 27 type Fourier-transformed infrared spectrometer (resolution: 2 cm<sup>-1</sup>, illumination: SiC Globar light, monochromator: Littrow prism, detector: RT-DLaTGS (Deutero L- $\alpha$ -Alanine Triglycine-Sulphate) type detector with KBr window) was used for identification of raw materials using spectrum comparison in wavenumber range of 4000-400 cm<sup>-1</sup>.

Specific surface area, pore volume and pore size distribution in the micropore (1.7-2 nm), mesopore (2–50 nm) and the macropore (50–100 nm) diameter ranges of the catalysts were determined by nitrogen adsorption/desorption isotherms tested by a Micromeritics ASAP 2000-type instrument. For analysis the samples (weight ~0.5-0.7 g) were previously outgassed in vacuum at 160 °C. Pretreatment of each sample was finished when vacuum reached less than 10  $\mu$ Torr. The surface areas of the samples were determined by the BET (Brunauer-Emmett-Teller) method from the corresponding nitrogen adsorption isotherm. The pore size distribution and volume values were calculated from nitrogen desorption isotherms using the BJH (Barret–Joyner–Halenda) model.

Composition of gaseous products was analyzed by gas-chromatography (GC) (DANI type GC instrument, programmed injector, flame ionized detector) using Rtx-1 PONA column (100 m x 0.25 mm, surface thickness of 0.5  $\mu$ m) and Rtx-5 PONA (5 m x 0.25 mm, surface thickness of 1  $\mu$ m). Sample was analyzed at isotherm conditions (T=30 °C). The temperature of injector and detector was 240 °C. For calibration gas mixture of defined composition was used.

Pyrolysis oil was analyzed also by DANI GC, using Rtx-1 dimethyl-polysiloxane capillary (30 m x 0.53 mm, thickness of 0.25  $\mu$ m) using the following temperature program: 40 °C for 5 minutes, then the temperature was elevated by 8 °C/min till 340 °C and it was kept at 340 °C for 20 min. Both injector and detector temperatures were 340 °C. Identification of GC peaks was based on retention time of standards and integrated peak area values of the gas chromatograms provided quantitative data of the GC analyses are.

### 3. Results and discussion

#### 3.1. Catalyst characterization

Table 1 summarizes the textural properties of the catalysts. These values were determined on the basis of the obtained adsorption/desorption isotherms. According to Table 1, addition of metals changed textural properties of ZSM-5. BET surface area ( $S_{\text{BET}}$ ), surface area of the micro pores ( $S_{\text{micro}}$ ) and micro pore volume ( $V_{\text{micro}}$ ) were decreased in each case, while BJH surface area ( $S_{\text{BJH}}$ ) and average pore diameter ( $D_{\text{av}}$ ) were increased, compared to unmodified ZSM-5 catalyst. By adding of iron BET surface area decreased the least (-2.8 %), with adding cerium it decreased to the greatest extent (-19.7 %). Opposite proportionality can be observed in the effects of the metals in case of BJH surface area. The pore volume between 1.7 and 300 nm increased mostly by the addition of tin (28.1 %), and decreased in only one case when the zeolite was modified by cerium (-1.9 %). Magnesium resulted the smallest reduce in the surface area of the micro pores and the micro pore volume (-12.5 % and -12.4 %, respectively), and the highest reduction was found with cerium (-27.5 % and -27.7 %, respectively). The average pore diameter increased to the highest extent by the effect of tin (10.3 %) and the least by cerium (2.9 %). According to this data it is declare that adding cerium and tin had the most influence on the textural properties of zeolites.

**Table 1** The surface area, pore volume and pore size of the catalysts

| Catalyst     | $S_{\text{BET}}$ (m <sup>2</sup> /g) | $S_{\text{BJH}}$ (m <sup>2</sup> /g) | Pore volume<br>$V_{1.7-300 \text{ nm}}$ (cm <sup>3</sup> /g) | $S_{\text{micro}}$<br>(m <sup>2</sup> /g) | $V_{\text{micro}}$ (cm <sup>3</sup> /g) | $D_{\text{av}}$ (nm) |
|--------------|--------------------------------------|--------------------------------------|--|---|---|----------------------|
| ZSM-5        | 355.4                                | 90.1                                 | 0.08508  | 221.1                                     | 0.10356                                 | 1.74                 |
| Zn/ZSM-5     | 350.8                                | 110.6                                | 0.10206  | 187.5                                     | 0.08729                                 | 1.80                 |
| Mg/ZSM-5     | 345.3                                | 109.2                                | 0.09994  | 193.5                                     | 0.09076                                 | 1.80                 |
| Fe(II)/ZSM-5 | 354.5                                | 111.7                                | 0.10428  | 190.6                                     | 0.08886                                 | 1.81                 |
| Sn/ZSM-5     | 318.9                                | 105.0                                | 0.10900  | 166.3                                     | 0.07741                                 | 1.92                 |
| Ce/ZSM-5     | 285.4                                | 91.9                                 | 0.08343  | 160.4                                     | 0.07485                                 | 1.79                 |

#### 3.2. Pyrolysis yields

The yields of the products of ELV decomposition are summarized in Fig2. It can be seen, that the raw materials were decomposed mainly into gases and pyrolysis oil. At the end of the pyrolysis 0.7-1.3 wt% solid residues were remain on the bottom of the reactor vessel. At 425 °C, the gas yield increased, while the yield of pyrolysis oil decreased following the order of Ce/ZSM-5 > Fe(II)/ZSM-5 > Zn/ZSM-5 > Mg/ZSM-5 > Sn/ZSM-5 catalyst. When the pyrolysis temperature was enhanced at 485 °C the obtained order was very similar: Ce/ZSM-5 > Zn/ZSM-5 > Fe(II)/ZSM-5 > Mg/ZSM-5 > Sn/ZSM-5. The maximum yield of pyrolysis oil and the minimum yield of gases over Sn/ZSM-5 catalyst were in both cases. At 425 °C these yields were 56.7 wt% and 42.6 wt%, and at the higher temperature there were 55.4 wt% and 43.9 wt%, respectively. On the other hand, the lowest yield of pyrolysis oil and the highest yield of gas were found by the using of Ce/ZSM-5 catalyst, with yields of 38.6 wt% and 60.6 wt% at 425 °C, and 45.2 wt% and 53.9 wt% at 485 °C, respectively. It was expected that these catalysts will result outstanding values, because these two metals have modified to the largest degree the properties of zeolites. Using of cerium impregnated catalyst generated the most gas that means that cerium had a big cracking effect. In contrast, tin had a slight cracking effect. Presumably this time thermal cracking reactions dominated during the pyrolysis.

It is clear that the yields of volatile products were almost the same in all cases, only the ratios of gases and liquids changed. At 485 °C the yields of gases decreased with using Fe/ZSM-5, Ce/ZSM-5 and Mg/ZSM-5, and small growth can be observed with Zn and Sn/ZSM-5 compared to the lower temperature. These changes were -8.4 %, -11.1 %, -4.7 %, 2.8 % and 3.0 %, respectively. Higher temperature is favorable for the intensive cracking of C-C, resulting mainly gases, however the opposite result was observed in our experiments. This is because at higher temperatures the higher boiling point components have become gaseous, and since the reactor system is open and continuously passed through the nitrogen, it took out these higher boiling point components to the refrigerator and separator so they can appeared in pyrolysis oil. If the system were closed, greater gas evolution would be observed at higher temperature.

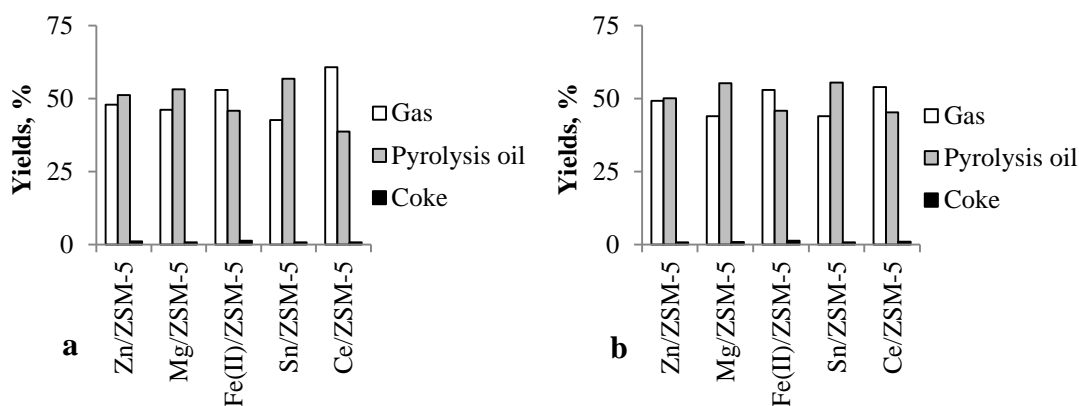


**Fig2** The yields of products (a, 425 °C; b, 485 °C)

### 3.3. Gases

The hydrocarbon compositions of gases are summarized in Fig3. and Fig4. Gases contain mainly C3-C5 hydrocarbons (88.7-91.9 wt%) as Fig3 shows. At 425 °C, with 0.3-3.0 wt% more C3-C5 hydrocarbons were generated than at 485 °C; while the amount of C1-C2 hydrocarbons (methane, ethane, ethane) increased with 4.7-52.4 % by enhance the temperature. The lowest growth (4.7 %) in C1-C2 gases yield was found in case of magnesium-impregnated zeolite, while the highest growing was observed with iron(II) and cerium, 40.5 % and 52.4 %, respectively. The Ce/ZSM-5 catalyst resulted 9,9 wt% C1-2 hydrocarbons yield.

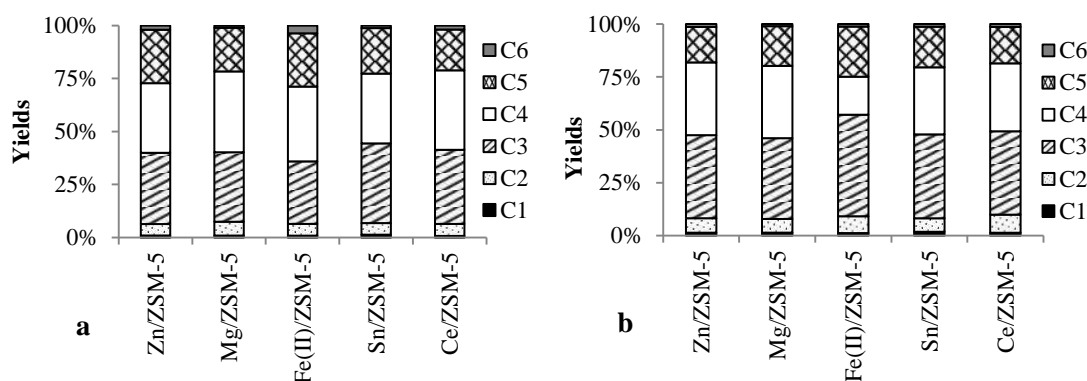


**Fig3** The composition of the gas products according to the carbon number (a, 425 °C; b, 485 °C)

It can be demonstrated on Fig4, that the gases consist of dominantly non-branched saturated hydrocarbons (11.1-15.1 wt%), unsaturated  $\alpha$ -olefins (44.2-66.0 wt%), and branched hydrocarbons (21.2-42.7 wt%). The yield of n-paraffins did not change significantly comparing the catalytic processes. The highest concentration of branched hydrocarbon was found by using of modified ZSM-5 zeolite with zinc at 425 °C and with magnesium at 485 °C; 42.7 wt% and 35.7 wt%, respectively. The highest yields of  $\alpha$ -olefins were obtained with Sn/ZSM-5 catalyst at 425 °C and Fe(II)/ZSM-5 catalyst at 485 °C; 51.2 wt% and 66.0 wt%, respectively. According to the results in case of Sn/ZSM-5 catalyst the temperature had minor effect on the gas composition, whilst used Fe(II)/ZSM-5 catalyst the proportions of  $\alpha$ -olefins and branched hydrocarbons changed more than 40 %.

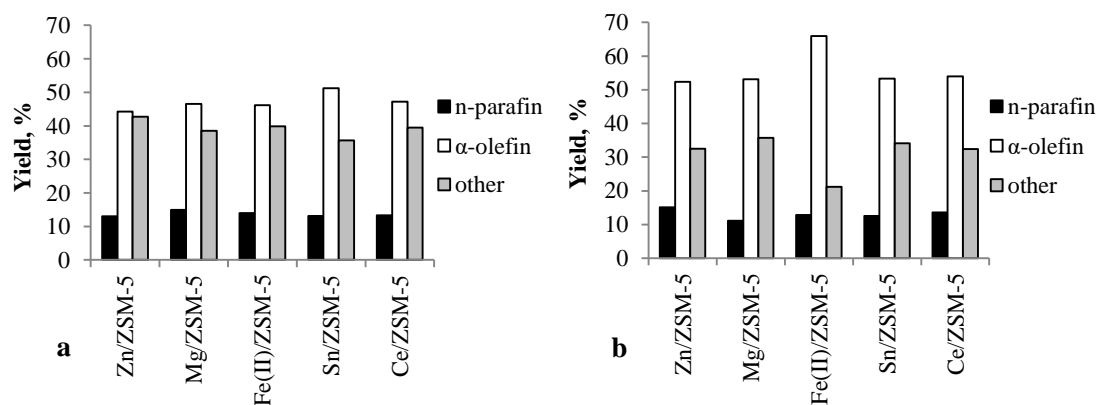


**Fig4** The hydrocarbon composition of the gas products (a, 425 °C; b, 485 °C)

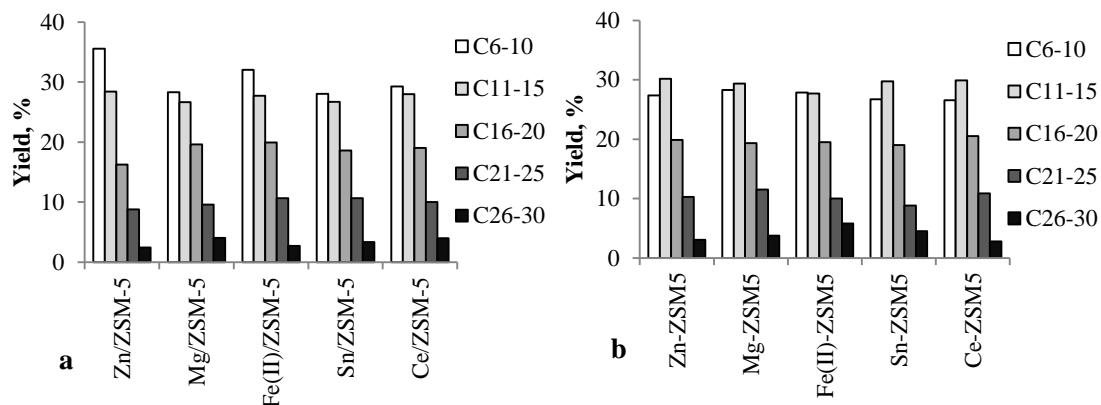
### 3.4. Pyrolysis oil

The concentration of C6-C30 hydrocarbons in pyrolysis oils have been listed in Table 4. Each sample contained high amount of C8 and C13 hydrocarbons; 10.4-13.8 wt% and 9.4-10.7 wt%, respectively. 7.7-12.7 wt% of the pyrolysis oil was C30+ hydrocarbons. At both temperatures with using of tin modified zeolite generated the most C30+ components. As Fig2 shows, the same catalyst produced the highest liquid product yields at both temperatures. Presumably, this catalyst had the lowest activity of cracking reactions.

Fig5 shows that pyrolysis oil consisted dominantly C6-C15 hydrocarbons (54.7-64.0 wt%). The highest concentration was 64 wt% with using of Zn/ZSM-5 catalyst. The concentration of the C6-C15 fraction during the pyrolysis at 425 °C increased following the order of Sn/ZSM-5, Mg/ZSM-5, Ce/ZSM-5, Fe(II)/ZSM-5 and Zn/ZSM-5 catalyst. At 485 °C the effects of the catalyst were less remarkable, because the C6-15 yield was 55.5-57.7 wt%, which can be attributed to the fact that at this temperature the thermal reactions became dominant.

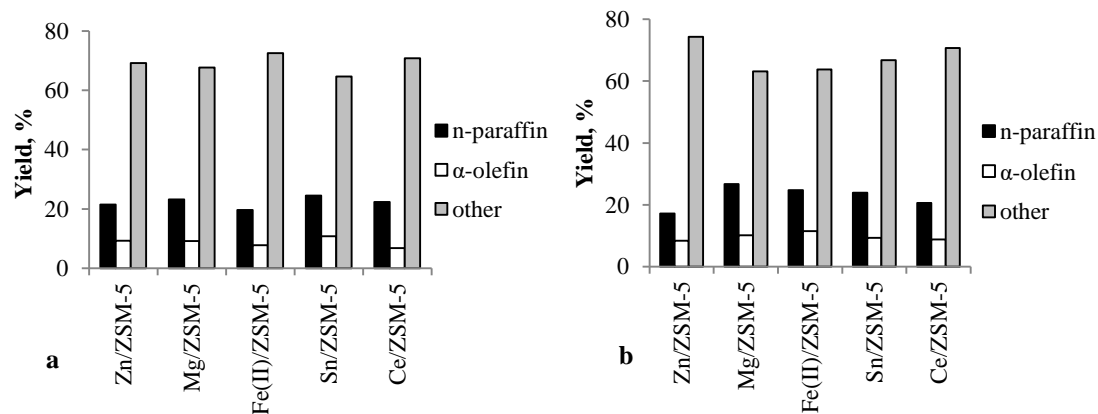
**Table 2** The composition of the pyrolysis oils as a function of the carbon number (the values in wt%)

| Component        | 425 °C      |             |                 |             |             | 485 °C      |             |                 |             |             |
|------------------|-------------|-------------|-----------------|-------------|-------------|-------------|-------------|-----------------|-------------|-------------|
|                  | Zn/<br>ZSM5 | Mg/<br>ZSM5 | Fe(II)/<br>ZSM5 | Sn/<br>ZSM5 | Ce/<br>ZSM5 | Zn/<br>ZSM5 | Mg/<br>ZSM5 | Fe(II)/<br>ZSM5 | Sn/<br>ZSM5 | Ce/<br>ZSM5 |
| C <sub>6</sub>   | 0.76        | 0.60        | 0.54            | 0.46        | 0.26        | 0.13        | 0.39        | 0.53            | 0.25        | 0.26        |
| C <sub>7</sub>   | 5.58        | 5.24        | 5.92            | 5.34        | 4.11        | 5.34        | 5.19        | 5.67            | 3.90        | 3.85        |
| C <sub>8</sub>   | 13.83       | 10.93       | 12.25           | 11.74       | 11.55       | 10.95       | 11.43       | 10.42           | 10.96       | 11.30       |
| C <sub>9</sub>   | 7.61        | 5.99        | 6.73            | 5.34        | 6.80        | 5.21        | 6.10        | 5.54            | 5.79        | 5.78        |
| C <sub>10</sub>  | 7.74        | 5.54        | 6.59            | 5.18        | 6.55        | 5.74        | 5.19        | 5.67            | 5.79        | 5.39        |
| C <sub>11</sub>  | 6.73        | 5.69        | 5.65            | 5.49        | 5.65        | 6.28        | 6.36        | 5.41            | 6.42        | 6.03        |
| C <sub>12</sub>  | 4.19        | 2.99        | 2.96            | 3.20        | 3.21        | 3.34        | 3.77        | 3.83            | 4.03        | 3.85        |
| C <sub>13</sub>  | 9.39        | 9.88        | 10.23           | 9.91        | 10.65       | 10.15       | 9.74        | 9.63            | 10.20       | 10.53       |
| C <sub>14</sub>  | 3.81        | 3.89        | 4.04            | 3.66        | 3.85        | 3.47        | 4.55        | 4.09            | 4.28        | 4.49        |
| C <sub>15</sub>  | 4.31        | 4.19        | 4.85            | 4.42        | 4.62        | 6.94        | 4.94        | 4.75            | 4.79        | 5.01        |
| C <sub>16</sub>  | 3.93        | 5.09        | 4.98            | 5.03        | 4.62        | 3.60        | 4.55        | 4.62            | 4.79        | 5.01        |
| C <sub>17</sub>  | 3.93        | 4.64        | 4.71            | 3.96        | 4.36        | 6.94        | 4.81        | 4.75            | 4.41        | 4.75        |
| C <sub>18</sub>  | 4.44        | 5.24        | 5.65            | 5.18        | 5.65        | 3.07        | 5.06        | 5.15            | 5.16        | 5.78        |
| C <sub>19</sub>  | 1.78        | 1.95        | 2.02            | 1.98        | 1.93        | 3.20        | 2.73        | 2.51            | 2.02        | 2.18        |
| C <sub>20</sub>  | 2.16        | 2.69        | 2.56            | 2.44        | 2.44        | 3.07        | 2.21        | 2.51            | 2.64        | 2.82        |
| C <sub>21</sub>  | 2.79        | 2.84        | 3.63            | 3.66        | 3.59        | 2.14        | 3.90        | 3.69            | 3.53        | 3.59        |
| C <sub>22</sub>  | 0.89        | 1.05        | 1.21            | 1.22        | 1.03        | 1.60        | 1.43        | 1.45            | 1.01        | 1.03        |
| C <sub>23</sub>  | 1.65        | 1.05        | 0.94            | 1.22        | 1.28        | 1.20        | 1.43        | 1.32            | 1.13        | 1.67        |
| C <sub>24</sub>  | 0.63        | 1.50        | 1.35            | 1.22        | 0.90        | 1.87        | 1.56        | 1.45            | 1.13        | 0.77        |
| C <sub>25</sub>  | 2.79        | 3.14        | 3.50            | 3.35        | 3.21        | 3.47        | 3.25        | 2.11            | 2.02        | 3.85        |
| C <sub>26</sub>  | 0.13        | 0.45        | 0.27            | 1.37        | 0.64        | 0.13        | 0.26        | 1.85            | 1.64        | 1.16        |
| C <sub>27</sub>  | 0.89        | 1.05        | 0.94            | 0.15        | 1.41        | 0.93        | 1.04        | 1.32            | 1.26        | 0.51        |
| C <sub>28</sub>  | 0.76        | 0.60        | 0.81            | 0.76        | 0.90        | 0.40        | 0.78        | 1.19            | 0.76        | 0.39        |
| C <sub>29</sub>  | 0.25        | 0.45        | 0.54            | 0.61        | 0.39        | 0.93        | 0.78        | 0.79            | 0.25        | 0.64        |
| C <sub>30</sub>  | 0.38        | 1.50        | 0.13            | 0.46        | 0.64        | 0.67        | 0.91        | 0.66            | 0.63        | 0.13        |
| C <sub>30+</sub> | 8.63        | 11.83       | 7.00            | 12.65       | 9.76        | 9.21        | 7.66        | 9.10            | 11.21       | 9.24        |



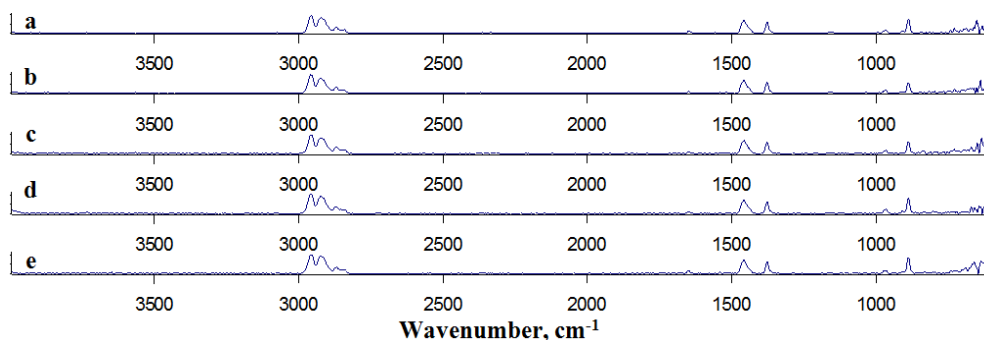
**Fig5** The composition of the pyrolysis oils according to the carbon number ranges (a, 425 °C; b, 485 °C)

Fig6 summarizes the composition of pyrolysis oils, such as n-saturated, n-unsaturated and other (branched and aromatics) compounds. According to results, increasing in temperature had significant effect on the change in the yield of these types of hydrocarbon when iron was used as impregnation agent. At 425 °C, this catalyst had the most significantly effect to the formation of the non-branched chain saturated hydrocarbon, which was 72.5 wt%. At the higher process temperature 25.9 % more n-paraffin generated, 47.6 % more  $\alpha$ -olefin and 12.2 % less branched hydrocarbon. The highest  $\alpha$ -olefin yield was obtained in this case, it was 11.5 wt%. Regarding n-paraffins, Mg/ZSM-5 resulted the highest yield of n-unsaturated compounds at 485 °C, it was 26.8 wt%. The high concentration of branched hydrocarbon was also the consequence of the high ratio of PP (42 %) in raw material. The chemical structure of PP contains ramifications; therefore dominantly branched hydrocarbons could be formed from them.



**Fig6** The composition of the pyrolysis oils (a, 425 °C; b, 485 °C)

Fig7 and Fig8 show the FTIR spectrum of pyrolysis oils in 4000-400  $\text{cm}^{-1}$  wave-number range, which refers to infrared activity in the range of 2800-3000  $\text{cm}^{-1}$ , 1300-1500  $\text{cm}^{-1}$  and 700-1000  $\text{cm}^{-1}$ .



**Fig7** The FTIR spectra of the obtained pyrolysis oil at 425 °C (a, Zn/ZSM-5; b, Mg/ZSM-5; c, Fe(II)/ZSM-5; d, Sn/ZSM-5; e, Ce/ZSM-5)

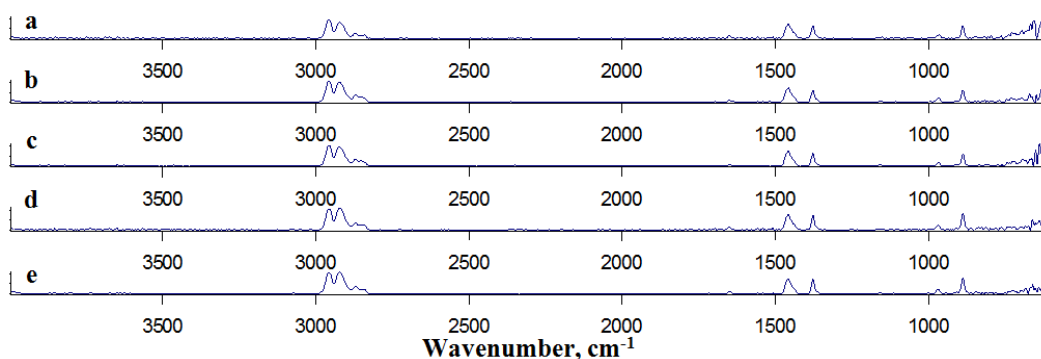


**Fig8** The FTIR spectra of the obtained pyrolysis oil at 485 °C (a, Zn/ZSM-5; b, Mg/ZSM-5; c, Fe(II)/ZSM-5; d, Sn/ZSM-5; e, Ce/ZSM-5)

Bands between 2800 and 3000  $\text{cm}^{-1}$  could be attributed to the symmetric and asymmetric C–H stretching vibration of  $-\text{CH}_2-$  ( $\nu_{\text{as}}\text{CH}_2$ ,  $\nu_{\text{s}}\text{CH}_2$ , 2926  $\text{cm}^{-1}$  and 2836  $\text{cm}^{-1}$ ) and  $-\text{CH}_3$  ( $\nu_{\text{as}}\text{CH}_3$ ,  $\nu_{\text{s}}\text{CH}_3$ , 2962 and 2872  $\text{cm}^{-1}$ ) groups. Comparing spectrum higher intensity of bands belongs to methyl group and lower intensity of bands belongs to methylene groups were found at the higher pyrolysis temperature. The infrared activity between 1470–1430  $\text{cm}^{-1}$  and 1400–1350  $\text{cm}^{-1}$  was the consequence of the asymmetric and symmetric deformation stretching of  $-\text{CH}_3$  groups. Unsaturated hydrocarbons show infrared activity between 800–1000  $\text{cm}^{-1}$ ; C–H stretching vibrations cause infrared bands. Results refers to the distribution of C=C bonds; vinyl, vinylidene and vinylene type double bonds result intensive adsorption bands at 910 and 990  $\text{cm}^{-1}$ , at 890  $\text{cm}^{-1}$  and at 956  $\text{cm}^{-1}$ , respectively.

### 3.5 Conclusion

In our experimental work pyrolysis of real ELV waste plastic was carried out in a batch reactor with using of different metal-modified ZSM-5 catalysts at 425 °C and at 485 °C. According to the product yields the Ce/ZSM-5 catalyst showed the highest activity for cracking reactions and Sn/ZSM-5 catalyst showed the least activity. Gas products contained mainly C3-C5 hydrocarbons (88.7-91.9 wt%) with big unsaturated  $\alpha$ -olefins content (44.2-66.0 wt%), but in the case of Ce/ZSM-5 catalyst it contained 9,9 wt% light (C1-2) hydrocarbons. The components in the pyrolysis oil were identified until C30, and this product consisted dominantly C6-C15 hydrocarbons (54.7-64.0 wt%).

### Acknowledgments

The authors express their gratitude to the National Office for Research and Innovation, within the framework of support for Hungarian-Indian (KTIA-DST) R&D&I co-operation program (TÉT\_13\_DST) (TÉT\_13\_DST-1-2014-0003).

## References

- [1] [http://www.plasticseurope.org/documents/document/20161014113313-plastics\\_the\\_facts\\_2016\\_final\\_version.pdf](http://www.plasticseurope.org/documents/document/20161014113313-plastics_the_facts_2016_final_version.pdf) (2017) Accessed 19 May 2017
- [2] European Parliament and the European Council, Directive 94/62/EC of the European Parliament and of the Council of 20 December 1994 on packaging and packaging waste, Off. J. Eur. Commun. L 365 (1994) 10-23.
- [3] European Parliament and the European Council, Directive 2000/53/EC of the European Parliament and of the Council of 18 September 2000 on end-of-life vehicles, Off. J. Eur. Commun. L 269 (2000) 34–42.
- [4] <http://ec.europa.eu/environment/waste/elv/> (2017) Accessed 19 May 2017
- [5] Vermeulen, I., Van Caneghem, J., Block, C., Baeyens, J., Vandecasteele, C.: Automotive shredder residue (ASR): reviewing its production from end-of-life vehicles (ELVs) and its recycling, energy or chemicals' valorization. *J. Hazard. Mater.* 190 (1), 8–27 (2011)
- [6] Samolada, M.C., Zabaniotou, A.A.: Potential application of pyrolysis for the effective valorisation of the end of life tires in Greece. *Environ. Dev.* (2012). doi: 10.1016/j.envdev.2012.08.004
- [7] Lin, K.-S., Chowdhury, S., Wang, Z.-P. Catalytic gasification of automotive shredder residues with hydrogen generation. *J. Power Sources* (2010). doi: 10.1016/j.jpowsour.2010.03.084
- [8] Ding, K., Zhong, Z., Zhang, B., Wang, J., Min, A., Ruan, R.: Catalytic pyrolysis of waste tire to produce valuable aromatic hydrocarbons: An analytical Py-GC/MS study. *J. Anal. Appl. Pyrolysis* (2016). doi: 10.1016/j.jaap.2016.10.023
- [9] Miandad, R., Barakat, M.A., Aburiazaiza, A.S., Rehan, M., Nizami, A.S.: Catalytic pyrolysis of plastic waste: A review. *Process Saf. Environ. Prot.* (2016). doi: 10.1016/j.psep.2016.06.022
- [10] Williams, P.T., Williams, E.A.: Fluidised bed pyrolysis of low density polyethylene to produce petrochemical feedstock. *J. Anal. Appl. Pyrol.* (1999). doi: 10.1016/S0165-2370(99)00011-X
- [11] Wong, S.L., Tuan Abdullah, T.A., Ngadi, N., Ahmad, A., Inuwa, I.M.: Parametric study on catalytic cracking of LDPE to liquid fuel over ZSM-5 zeolite. *Energy. Convers. Manage.* (2016). doi: 10.1016/j.enconman.2016.06.009
- [12] Ratnasari, D.K., Nahil, M.A., Williams, P.T.: Catalytic pyrolysis of waste plastics using staged catalysis for production of gasoline range hydrocarbon oils. *J. Anal. Appl. Pyrol.* (2017). doi: 10.1016/j.jaap.2016.12.027
- [13] López, A., Marco, I., Caballero, B.M., Adrados, A., Laresgoiti, M.F.: Deactivation and regeneration of ZSM-5 zeolite in catalytic pyrolysis of plastic wastes. *Waste Manage.* (2011). doi: 10.1016/j.wasman.2011.04.004
- [14] López, A., Marco, I., Caballero, B.M., Laresgoiti, M.F., Adrados, A., Aranzabal, A.: Catalytic pyrolysis of plastic wastes with two different types of catalysts: ZSM-5 zeolite and Red Mud. *Appl. Catal. B: Environ.* (2011). doi: 10.1016/j.apcatb.2011.03.030
- [15] Hoff, T.C., Gardner, D.W., Thilakarathne, R., Proano-Aviles, J., Brown, R.C., Tessonnier, J.-P.: Elucidating the effect of desilication on aluminum-rich ZSM-5 zeolite and its

- consequences on biomass catalytic fast pyrolysis, *Appl. Catal. A: Gen.* (2017). doi: 10.1016/j.apcata.2016.10.009
- [16] Wu, C., Williams, P.T.: Ni/CeO<sub>2</sub>/ZSM-5 catalysts for the production of hydrogen from the pyrolysis–gasification of polypropylene. *Int. J. Hydrogen Energy* (2009). doi: 10.1016/j.ijhydene.2009.05.121
- [17] Elbaba, I.F., Wu, C., Williams, P.T.: Hydrogen production from the pyrolysis/gasification of waste tyres with a nickel/cerium catalyst. *Int. J. Hydrogen Energy* (2011). doi: 10.1016/j.ijhydene.2011.02.135
- [18] Li, X., Shen, B., Xu, C.: Interaction of titanium and iron oxide with ZSM-5 to tune the catalytic cracking of hydrocarbons. *Appl. Catal. A: Gen.* (2010). doi: 10.1016/j.apcata.2009.12.033
- [19] Sun, L., Zhang, X., Chen, L., Zhao, B., Yang, S., Xie, X.: Comparison of catalytic fast pyrolysis of biomass to aromatic hydrocarbons over ZSM-5 and Fe/ZSM-5 catalysts. *J. Anal. Appl. Pyrol.* (2016). doi: 10.1016/j.jaap.2016.08.015
- [20] Ji, X., Liu, B., Ma, W., Chen, G., Yan, B., Cheng, Z.: Effect of MgO promoter on Ni-Mg/ZSM-5 catalysts for catalytic pyrolysis of lipid-extracted residue of *Tribonema minus*. *J. Anal. Appl. Pyrol.* (2017). doi: 10.1016/j.jaap.2016.10.032
- [21] Wang, L., Lei, H., Bu, Q., Ren, S., Wei, Y., Zhu, L., Zhang, X., Liu, Y., Yadavalli, G., Lee, J., Chen, S., Tang, J.: Aromatic hydrocarbons production from ex situ catalysis of pyrolysis vapor over Zinc modified ZSM-5 in a packed-bed catalysis coupled with microwave pyrolysis reactor. *Fuel* (2014). doi: 10.1016/j.fuel.2014.03.052
- [22] Zhao, X., Wei, L., Cheng, S., Huang, Y., Yu, Y., Julson, J.: Catalytic cracking of camelina oil for hydrocarbon biofuel over ZSM-5-Zn catalyst. *Fuel Process. Technol.* (2015). doi: 10.1016/j.fuproc.2015.07.033